Stem Cell Reports, Volume *8*

Supplemental Information

SCA-1 Expression Level Identifies Quiescent Hematopoietic Stem and Progenitor Cells

Mina N.F. Morcos, Kristina B. Schoedel, Anja Hoppe, Rayk Behrendt, Onur Basak, Hans C. Clevers, Axel Roers, and Alexander Gerbaulet

Figure S1

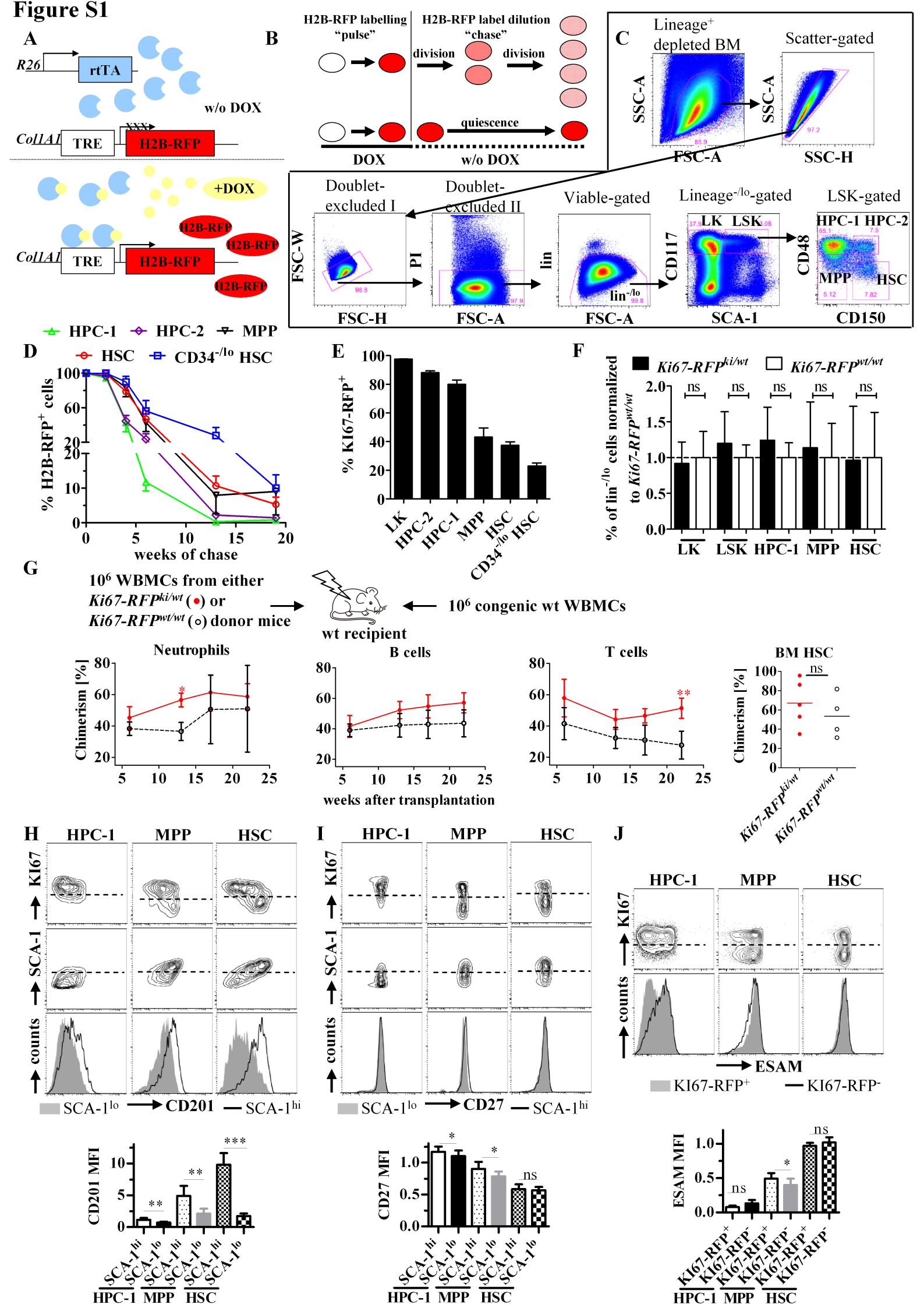
A
R26
rtTA
w/o DOX
Col1A1
TRE
H2B-RFP
+DOX
B
H2B-RFP labelling "pulse"
H2B-RFP label dilution "chase"
division
division
quiescence
DOX
w/o DOX
C
Lineage+ depleted BM
Scatter-gated
SSC-A
FSC-A
SSC-H
Doublet-excluded I
Doublet-excluded II
Viable-gated
Lineage-/lo-gated
LSK-gated
FSC-W
FSC-H
PI
lin
lin-/lo
CD117
LK
LSK
SCA-1
CD48
HPC-1
HPC-2
MPP
HSC
CD150
HPC-1
HPC-2
MPP
HSC
D
HSC
CD34-/lo HSC
% H2B-RFP+ cells
weeks of chase
E
% KI67-RFP+
LK
HPC-2
HPC-1
MPP
HSC
CD34-/lo HSC
F
Ki67-RFPki/wt
Ki67-RFPwt/wt
% of lin-/lo cells normalized to Ki67-RFPwt/wt
ns
LK
LSK
HPC-1
MPP
HSC
G
10⁶ WBMCs from either Ki67-RFPki/wt (•) or Ki67-RFPwt/wt (○) donor mice
10⁶ congenic wt WBMCs
wt recipient
Neutrophils
B cells
T cells
BM HSC
Chimerism [%]
weeks after transplantation
Ki67-RFPki/wt
Ki67-RFPwt/wt
H
HPC-1
MPP
HSC
KI67
SCA-1
counts
SCA-1lo
CD201
SCA-1hi
I
HPC-1
MPP
HSC
KI67
SCA-1
counts
SCA-1lo
CD27
SCA-1hi
J
HPC-1
MPP
HSC
KI67
counts
ESAM
KI67-RFP+
KI67-RFP-
CD201 MFI
CD27 MFI
ESAM MFI
SCA-1hi
SCA-1lo
HPC-1
MPP
HSC
KI67-RFP+
KI67-RFP-
ns

Figure S1. Mouse models for identification of quiescent hematopoietic stem and progenitor cells (related to Figure 1).

A Scheme of the *R26*^{rtTA}/*Col1A1*$^{H2B\text{-}RFP}$ mouse model. In the absence of doxycycline (DOX, yellow circles), the ubiquitously expressed reverse tetracycline transactivator (rtTA, blue circles) is unable to bind to tetracycline-responsive elements (TRE) of the TET-operon resulting in no or low level background expression of histone 2B-red fluorescent fusion protein (H2B-RFP). Systemic DOX administration results in massive induction of H2B-RFP (red ellipses) expression in all cells. **B** Scheme of H2B-RFP induction and dilution of the label by cell divisions. DOX induction leads to accumulation of H2B-RFP fusion protein ("pulse" period), while after DOX withdrawal ("chase") each cell division results in 50% dilution of H2B-RFP fluorescence. In contrast to this, non-dividing cells retain the H2B-RFP label. Note that the slow cell cycle-independent decay of the H2B-RFP protein was neglected in the scheme. **C** HSPC gating and sorting strategy adapted from Kiel et al., Cell, 2005. Representative dot plots of lineage-depleted WBMCs from a B6 wt mouse (LK, Lin$^{-/lo}$SCA-1^{-}CD117^{+}; LSK, Lin$^{-/lo}$SCA-1^{+}CD117^{+}; HPC-1, LSK CD48^{hi}CD150^{-}; HPC-2, LSK CD48^{hi}CD150^{+}; MPP, LSK CD48$^{-/lo}$CD150^{-}; HSC, LSK CD48$^{-/lo}$CD150^{+}; FSC, forward scatter; SSC, side scatter; PI, Propidium iodide; lin, hematopoietic lineage antigens). **D** *R26*^{rtTA}/*Col1A1*$^{H2B\text{-}RFP}$ mice (*R26* zygosity either *R26*$^{rtTA/wt}$ or *R26*$^{rtTA/rtTA}$, *Col1A1* zygosity either *Col1A1*$^{H2B\text{-}RFP/wt}$ or *Col1A1*$^{H2B\text{-}RFP/H2B\text{-}RFP}$) were DOX-pulsed for 8 weeks, chased for 0 (n=3), 2 (n=1), 4 (n=2), 6 (n=4), 13 (n=8) or 19 (n=9) weeks and BM was analyzed by flow cytometry for retention of H2B-RFP. Mean frequencies of H2B-RFP^{+} cells (± SD) among HSPC populations are shown (for gating see Figure S1C; CD34$^{-/lo}$ HSC, LSK CD48$^{-/lo}$CD150^{+}CD34$^{-/lo}$). The H2B-RFP^{+} gate was set using *R26*^{wt}/*Col1A1*$^{H2B\text{-}RFP}$ mice in order to control for the low level of background H2B-RFP expression from the *Col1A1*$^{H2B\text{-}RFP}$ allele.

E Mean frequencies (± SD) of KI67-RFP^{+} cells among BM HSPCs isolated from *Ki67-RFP*$^{ki/wt}$ mice (n=4) were analyzed by flow cytometry (KI67-RFP^{+} gate was set according to *Ki67-RFP*$^{wt/wt}$ controls; for HSPC gating see Figure S1C; CD34$^{-/lo}$ HSC, LSK CD48$^{-/lo}$CD150^{+}CD34$^{-/lo}$).

F BM HSPC population size of *Ki67-RFP*$^{ki/wt}$ (n=4) and *Ki67-RFP*$^{wt/wt}$ (n=3) mice was determined (mean frequencies (± SD) among lineage depleted BM cells are shown, mean frequencies of *Ki67-RFP*$^{wt/wt}$ mice were normalized to 1 (dotted line), significance was calculated by unpaired Student´s t-test with Bonferroni-Holm error correction).

G 10^6 WBMCs from either *Ki67-RFP*$^{ki/wt}$ (red circles) or *Ki67-RFP*$^{wt/wt}$ (black circles) mice were each mixed with 10^6 competitor B6.CD45.1 WBMCs and transplanted into lethally irradiated B6.CD45.1/.2 recipients (n=4-5 / per donor genotype). PB neutrophil, B- and T-lymphocyte chimerism was analyzed (mean ± SD are shown, significance was calculated with repeated measure two way ANOVA and Bonferroni error correction, only significant results are indicated). BM HSC (LSK CD48$^{-/lo}$CD150^{+}) chimerism of recipient mice was analyzed 23 weeks after transplantation (individual mice and means (bars) are shown, significance was calculated by unpaired Student´s t-test).

H BM of *Ki67-RFP*$^{ki/wt}$ mice (n=6) was analyzed by flow cytometry. Representative contour plots of HPCs-1 (LSK CD48^{hi}CD150^{-}), MPPs (LSK CD48$^{-/lo}$CD150^{-}) and HSCs (LSK CD48$^{-/lo}$CD150^{+}) are shown. Upper row depicts CD201 (EPCR) against KI67-RFP expression (dotted lines show threshold for KI67-RFP gating, set according to *Ki67-RFP*$^{wt/wt}$ control). Middle row shows CD201 against SCA-1 expression (dotted lines show threshold for arbitrary SCA-1^{hi} and SCA-1^{lo} gating). Lower row displays representative histograms of CD201 expression by either SCA-1^{lo} (solid grey histograms) or SCA-1^{hi} (black lines) cells among the respective parental HSPC population. Lower data plot quantifies CD201 expression of HSPC populations separated by SCA-1 expression level. CD201 MFI was normalized to the mean MFI of the total LSK population, which was set to 1 (means ± SD are shown, significance was calculated by paired Student´s t-test and Bonferroni-Holm error correction).

I BM of *Ki67-RFP*$^{ki/wt}$ mice (n=6) was analyzed by flow cytometry for expression of CD27 among HSPCs. Display, normalization and statistical analysis of data was performed as in Figure S1H.

J BM of *Ki67-RFP*$^{ki/wt}$ mice (n=4) was analyzed by flow cytometry for ESAM and KI67-RFP expression. Representative contour plots of HPCs-1 (LSK CD48^{hi}CD150^{-}), MPPs (LSK CD48$^{-/lo}$CD150^{-}) and HSCs (LSK CD48$^{-/lo}$CD150^{+}) are shown (upper row, dotted lines show threshold for KI67-RFP gating). Lower row compares ESAM expression between KI67-RFP^{+} (solid grey histograms) and KI67-RFP^{-} (black lines) cells among the respective parental population. Lower data plot depicts ESAM expression of HSPC populations separated by KI67-RFP expression. ESAM MFI was normalized to the mean MFI of the total HSC population, which was set to 1 (mean ± SD are shown, significance was calculated by paired Student´s t-test and Bonferroni-Holm error correction).

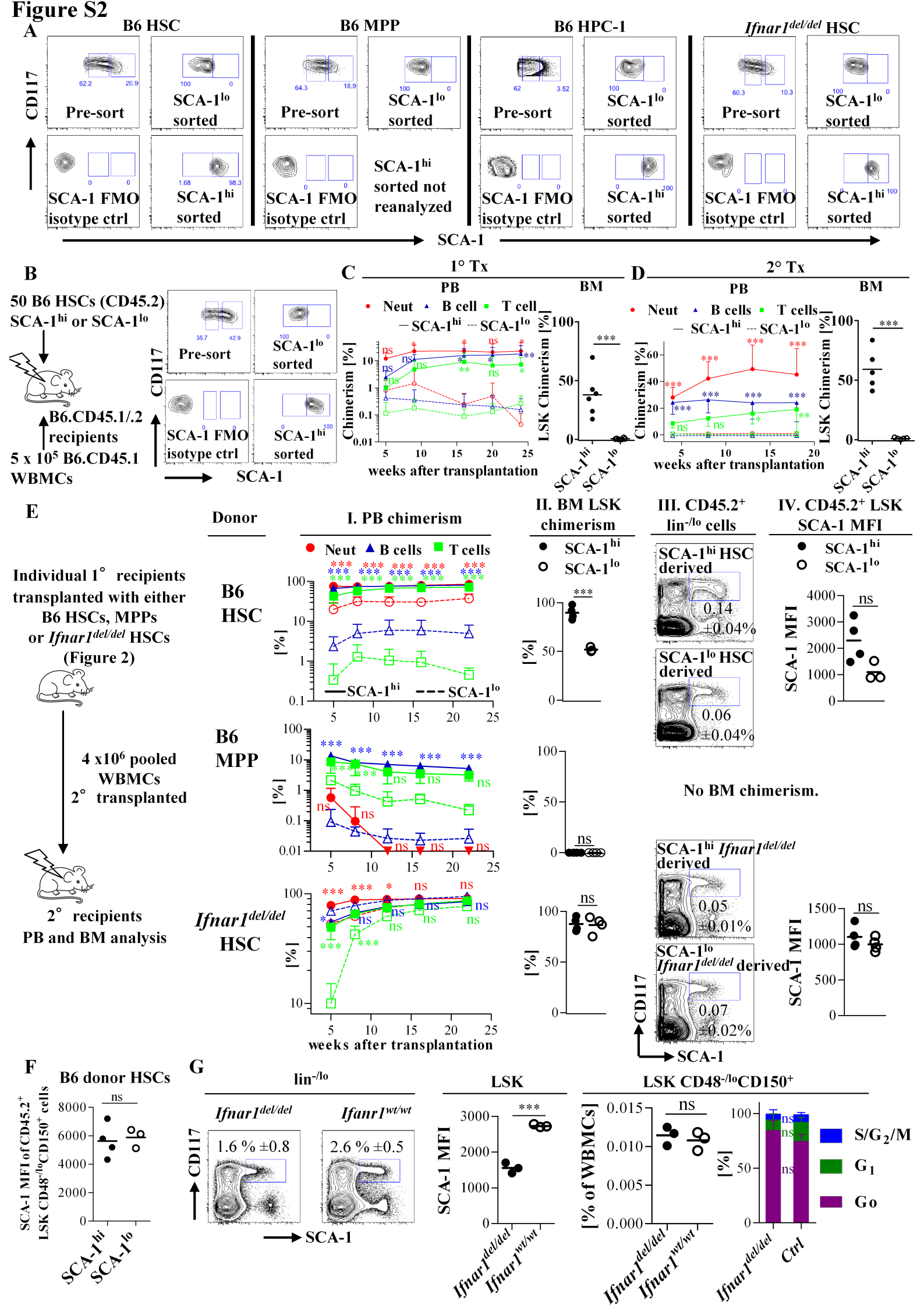
Figure S2
A
B6 HSC
B6 MPP
B6 HPC-1
Ifnar1del/del HSC
CD117
Pre-sort
SCA-1lo sorted
SCA-1 FMO isotype ctrl
SCA-1hi sorted
SCA-1hi sorted not reanalyzed
SCA-1
B
50 B6 HSCs (CD45.2)
SCA-1hi or SCA-1lo
B6.CD45.1/.2 recipients
5 x 10^5 B6.CD45.1 WBMCs
C
1° Tx
PB
BM
Neut
B cell
T cell
SCA-1hi
SCA-1lo
Chimerism [%]
LSK Chimerism [%]
weeks after transplantation
D
2° Tx
E
Donor
I. PB chimerism
II. BM LSK chimerism
III. CD45.2+ lin-/lo cells
IV. CD45.2+ LSK SCA-1 MFI
Individual 1° recipients transplanted with either B6 HSCs, MPPs or Ifnar1del/del HSCs (Figure 2)
B6 HSC
B6 MPP
Ifnar1del/del HSC
4 x10^6 pooled WBMCs 2° transplanted
2° recipients PB and BM analysis
SCA-1hi HSC derived
SCA-1lo HSC derived
0.14 ±0.04%
0.06 ±0.04%
No BM chimerism.
SCA-1hi Ifnar1del/del derived
SCA-1lo Ifnar1del/del derived
0.05 ±0.01%
0.07 ±0.02%
SCA-1 MFI
F
B6 donor HSCs
SCA-1 MFI of CD45.2+ LSK CD48-/loCD150+ cells
G
lin-/lo
LSK
LSK CD48-/loCD150+
Ifnar1del/del
Ifanr1wt/wt
1.6 % ±0.8
2.6 % ±0.5
[% of WBMCs]
S/G2/M
G1
Go
Ctrl

Figure S2. Purification and transplantation of hematopoietic stem and progenitor cells according to SCA-1 expression levels (related to Figure 2).

A Contour plots show purification and reanalysis of either SCA-1^{hi} or SCA-1^{lo} HSPC donor populations transplanted in the experiment shown in Figure 2. SCA-1 Fluorescence-minus-one (FMO) isotype controls confirmed that all sorted populations were indeed SCA-1^{+}. Reanalysis of the SCA-1^{hi} sorted MPP population was not performed due to recovery of an insufficient cell number.

B B6 HSCs (LSK CD48$^{-/lo}$CD150^{+}) were fractionated according to SCA-1 expression and 50 cells were transplanted together with 5x10^{5} B6.CD45.1 competitor WBMCs into lethally irradiated B6.CD45.1/.2 recipients. Contour plots show purification and reanalysis of SCA-1^{hi} or SCA-1^{lo} donor HSCs,

C PB chimerism of primary (1° Tx) recipient mice (n= 6 / group, shown in Figure S2B) was monitored longitudinally (red circles, neutrophils; blue triangles, B cells; green boxes, T cells, continuous lines SCA-1^{hi} donor HSCs, dotted lines SCA-1^{lo} donor HSCs, means ± SD are shown, significance was calculated with repeated measure two way ANOVA with Bonferroni error correction). BM analysis of recipient mice revealed LSK donor chimerism (individual recipients and means are shown, unpaired Student´s t-test).

D 4x10^{6} WBMCs from pooled 1° recipient mice shown in Figure S2C were secondarily transplanted (2° Tx) into lethally irradiated recipients (n=5 / group) and PB and BM LSK chimerism (as in S2C) were analyzed.

E 4x10^{6} pooled WBMCs from 1° recipient mice from the experiment shown in Figure 2 were secondarily transplanted (2° Tx) into lethally irradiated recipients (n=3-4/group). Display and analysis of secondary recipient data is similar to Figure 2. **Column I.** depicts PB chimerism analysis (red circles, neutrophils; blue triangles, B cells; green boxes, T cells, continuous lines SCA-1^{hi} donor cells, dotted lines SCA-1^{lo} donor cells, means ± SD are shown, significance was calculated with repeated measure two way ANOVA with Bonferroni error correction). 2° transplantation of recipients that received SCA-1^{lo} MPP donor cells did not result in detectable neutrophil chimerism, while 2° recipients of SCA-1^{hi} MPP transplanted mice initially displayed low neutrophil chimerism, but neutrophil reconstitution was completely lacking after 12 weeks of 2° transplantation (indicated by inverted triangles on x-axis). **Column II.** depicts BM LSK chimerism of secondary recipients (individual mice and means are shown, unpaired Student´s t test). **Column III.** shows representative examples of contour plots of donor-derived (CD45.2^{+}) lin$^{-/lo}$ cells (mean frequencies ± SD of CD45.2^{+} LSK cells among total WBMCs are shown). **Column IV.** depicts SCA-1 MFI of donor-derived LSK cells (individual secondary recipients and means are shown, unpaired Student´s t test).

F SCA-1 MFI of the donor-derived (CD45.2^{+}) HSCs isolated from primary recipients (shown in Figure 2), which were transplanted with B6 HSCs, was analyzed (individuals and means are displayed, unpaired Student´s t test).

G WBMCs isolated from *Ifnar1*$^{del/del}$ or *Ifnar1*$^{wt/wt}$ mice (n=3/genotype) were analyzed by flow cytometry. The frequency of LSK cells among lin$^{-/lo}$ population (left, representative contour plots, mean ±SD) is displayed. SCA-1 MFI of LSK cells (middle data plot, individual mice and means, significance assessed by unpaired Student´s t test) was determined. The frequency of LSK CD48$^{-/lo}$CD150^{+} cells among WBMCs was unchanged in *Ifnar1*$^{del/del}$ mice compared to *Ifnar1*$^{wt/wt}$ controls (right data panel, individual mice and means are shown, significance calculated by unpaired Student´s t test). The proportion of LSK CD48$^{-/lo}$CD150^{+} cells in different cell cycle phases (G_0, G_1, S/G_2/M) in *Ifnar1*$^{del/del}$ (n=5) and control mice (genotype either *Ifnar1*$^{wt/del}$ *or Ifnar1*$^{wt/wt}$, n=4) was analyzed (mean ± SD, significance calculated by unpaired Student´s t test with Bonferroni-Holm error correction).

Table S1

Epitope	*Clone*	*Manufacturer*
CD117	2B8, 3C11	eBioscience, Miltenyi
CD11b	M1/70	eBioscience
CD135	A2F10	eBioscience
CD150	TC15-12F12.2	Biolegend
CD16/32	93	Biolegend
CD19	eBio1D3	eBioscience
CD27	LG.3A10	Biolegend
CD201 (EPCR)	eBio1560	eBioscience
CD34	RAM34	eBioscience
CD3e	145-2C11, eBio500A2	eBioscience
CD4	GK1.5	eBioscience
CD45.1	A20	eBioscience
CD45.2	104	eBioscience
CD45R (B220)	RA3-6B2	eBioscience
CD48	HM48-1	BD Biosciences
CD8a	53-6.7	eBioscience
ESAM	1G8/ESAM	Biolegend
GR-1 (LY-6C/G)	RB6-8C5	eBioscience
KI67	B56	BD Biosciences
NK1.1	PK136	eBioscience
SCA-1 (LY-6A/E)	D7	eBioscience
TER119	TER-119	eBioscience

Table S1
Overview of monoclonal antibodies used for flow cytometry.